Aerotaxy-grown GaAs nanowires using Ga seed particles

Eric Ceccarelli

LUNDS UNIVERSITET

Supervisor: Dr. Martin Magnusson
Co-supervisor: Sudhakar Sivakumar

Thesis submitted for the degree of
Master in Material Science

Faculty of science
Department of physics
Solid state physics

May 2021

Acknowledgments

I firstly would like to thank my supervisor Dr. Martin Magnusson for suggesting this topic to me and for the guidance he provided during this work.

I would also like to thank my co-supervisor Sudhakar Sivakumar for teaching me how to operate the aerotaxy tool and always being available whenever I ran into problems in the lab.

Lastly I would like to thank Bengt Meuller for fixing problems with the tool whenever it did not operate as intended.

Abstract

Aerotaxy offers an alternative method for the manufacturing of semiconductor nanowires. Instead of seeding growth on an expensive substrate, aerosol seed particles act as the catalyst for the Vapor–Liquid–Solid growth in a hot flow through reactor.

This thesis investigates the possibility of self-seeded GaAs nanowires grown from Ga seed particles replacing the regularly employed Au, hence eliminating potential impurities in the nanowire crystal lattice caused by the foreign seed particle material and not least dramatically reducing production costs.

The influence of reactor temperature, seed particle diameter and precursor flows on the morphology of the nanowires was investigated. It is found that a strongly tapered morphology is unavoidable despite extensive parameter exploration.

The seed particle size is discovered to strongly impact the nanowires' morphology, causing prominent kinking for seed particles diameters less than 50 nm in diameter and strongly affecting the wires length. The nanowires diameter is found to increase with the reactor temperature, while the length remains constant. Different precursor flows and V/III ratios were extensively explored, and their effect on the nanowires' morphology is discussed in detail. Preliminary results on Ga(As)P nanowires grown from Ga seed particles are also presented.

This explorative study presents a successful investigation of self-seeded nanowire growth using aerotaxy, potentially paving the way for future self seeded growth techniques.

Contents

1 Introduction

Semiconductor devices are essential for most of the technologies which society relies on. They are the basic building block of electronics, for transistors, light-emitting diodes or solar cells. Due to the relevance and great demand in this field, semiconductor devices are rapidly evolving and have been for decades. A perfect example of this phenomenon is Moore's law which states that every two years the number of transistors on a chip doubles. This law has been undeniably correct since 1965 and remains valid to this day. However, as devices are scaled down, new challenges emerge, for example the spatial accuracy of processing methods or even quantum effects like quantum tunneling, which could impact the device's performance [1]. The further miniaturization of devices is therefore insufficient to keep up with the rapidly growing demand for innovation, hence other options need to be considered. A proposed alternative solution is to explore different structures and materials, more specifically one dimensional nanostructures.

One dimensional nanostructures are amongst the most promising research topics in semiconductor physics, and due to their outstanding opto-electronic properties, they have captured the interest of numerous other fields of physics [2]. In particular focus are III-V type material nanowires, such as InGaAs, GaAs and GaAsP. These types of nanowires present high carrier mobility and band gap tunability giving them potential applications in the development of several opto-electronic devices [3]. One examples is in transistor technology, more specifically in NanoWire Field Effect Transistors (NWFET) which employ the wires as channels between source and drain allowing for a precise control of the drain current through the use of a gate voltage [4, 5]. Another application is in multi junction solar cells, which are composed of multiple pn-junctions fabricated from different materials allowing for the capture of photons in a wider solar spectrum, therefore enhancing the performance of the solar cell [6]. A schematic of these two devices is displayed in figure 1. Nanowires are used for this purpose since their composition is more easily controlled and manipulated, as compared to traditional epitaxy, allowing for the stacking of lattice mismatched materials [7]. However the commercialization of such nanowires is limited by current manufacturing methods, which do not allow for large scale and cost efficient manufacturing.

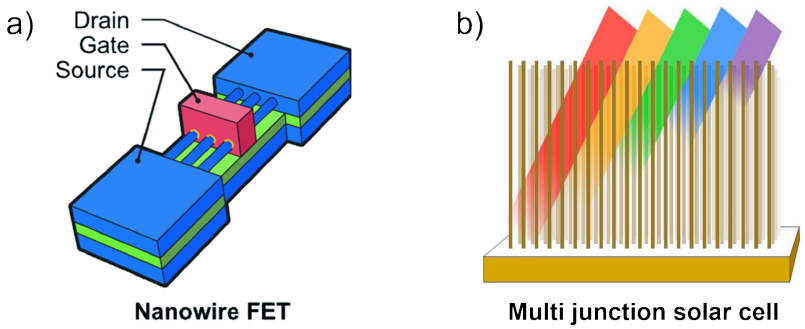

Figure 1: a) Schematic of nanowire FET [8], b) schematic of multi junction solar cell [9].

The Vapor–Liquid–Solid (VLS) mechanism is the most commonly adopted method for the growth of nanowires [10, 11, 12]. As the name suggests, this mechanism involves the

three states of matter: The precursors are supplied to the system in vapor form, they are then channeled in a liquid catalytic seed particle which allows growth in a specific direction, and therefore creates a solid crystalline structure i.e. the nanowire. Several manufacturing techniques rely on VLS, examples of which are molecular beam epitaxy (MBE) [13], chemical beam epitaxy (CBE) [14], pulsed laser ablation (PLA) [15] and metalorganic vapor phase epitaxy (MOVPE), which is the most frequently used and is explained in section 2.2.2. Such methods are expensive and generally slow, due to expensive substrates and only allow for a limited amount of nanowires to be grown with each batch.

In this thesis an alternative nanowire growth method, called Aerotaxy is investigated, which could potentially offer a more economic and time efficient manufacturing technique, while still having high control over the nanowire composition and structure. This method is based on utilizing aerosol catalytic nanoparticles which are mixed with a III-V precursor flux in a hot flow-through reactor. The rate of growth is about 1 μm/s and occurs in the [111] direction. This method allows for rapid growth without the need for an expensive substrate.

2 Theory and equipment

In aerotaxy, the wire growth is seeded by catalytic nanoparticles which are suspended in a gas, hence fulfilling the definition of an aerosol. The setup can be divided into two main parts: the first one is the aerosol section, where the seed particles are created and processed; and the second part is the reactor section, where the epitaxial growth takes place. The first section of this chapter presents the theory and tools behind the aerosol generation in the experiment, while the second part mainly focuses around the theory behind the epitaxial growth, which takes place in the reactor.

2.1 Aerosol

An aerosol is defined as particles or droplets, generally between 1 nm and 1 mm in diameter, suspended in a gas. Aerosols have applications in several fields, for example in medicine to study and treat pulmonary diseases, in combustion technology where fuel can be aerosol, or in our case for the fabrication of nanostructures.

Aerosol particles can be created with several methods. Examples are laser ablation, which utilizes a series of laser pulses directed on a metal [16]; Arc evaporation, in which a controlled d.c. current is used to evaporate metal atoms from a liquid metal pool [17]; or the method which is adopted in this thesis, called the evaporation/condensation method. This technique is based on the thermal evaporation of a metal, which after a certain temperature threshold will supersaturate the gas around it causing nucleation events when cooling while exiting the furnace, creating nanoparticles.

The nucleation of a material in a gas can be classified as either homogeneous or heterogeneous and is best described by the Classical Nucleation Theory (CNT) [18]. The nucleation rate R, in the homogeneous case, is described by the equation

$$R = \rho Z j \exp\Big(\frac{-\Delta G}{kT}\Big). \tag{1}$$

Here ρ is the number of possible nucleation sites, j is the rate of molecules getting attached to the nucleus, kT is the thermal energy, ΔG is the free energy cost for the critical nucleus creation and Z is called the Zeldovich factor which describes the probability for a nucleus to not dissolve before contributing to the particle creation. For heterogeneous nucleation the free energy cost ΔG is much lower than for homogeneous nucleation and therefore is more frequent. However it is not ideal for nanoparticle creation since it relies on nucleation upon an impurity or surface.

Homogeneous nucleation is further limited by the Kelvin effect, which describes the vapor pressure for curved surfaces compared to flat ones. It expresses the saturation ratio of the vapor p/p_s as an exponential factor

$$\frac{p}{p_s} = exp\Big(\frac{4\gamma V_m}{RT d^*}\Big), \tag{2}$$

where γ is the surface tension, V_m is the molar volume and d^* is the droplet's diameter, also called Kelvin diameter.

To better understand this equation we can think of an example. If the vapor is cooled, the saturation ratio will increase, and since we can consider γ and V_m as constant, the Kelvin diameter will decrease along with the temperature T. Since this Kelvin diameter indicates the size of a particle which would not evaporate under these conditions, its decrease will allow the creation and growth of smaller molecules. However, in theory, for very small Kelvin diameters, the saturation pressure is very high which would cause the particle to instantly evaporate. In practice several clusters can form momentarily, hence aiding nucleation.

2.1.1 Particle processing

The particles created using the evaporation/condensation method are most often not perfectly spherical but form agglomerates of smaller particles. This is due to random collisions between newly created particles which get attached to each other and would be considered as a single particle by the components in the tool. Such particles are not ideal as seeds for the wire growth, and must therefore be compacted into more spherical shapes. This is usually done through a sintering process which reshapes the particles as shown in figure 2.

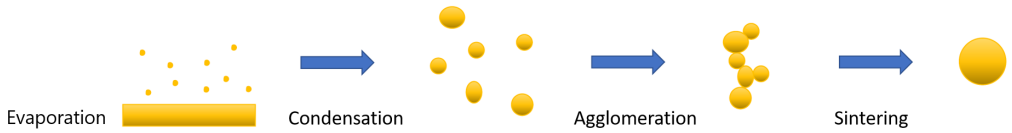

Figure 2: Each step for the aerosol particles from evaporation to sintering. The particles are at the nanometer scale.

The sintering temperature needs to be within a certain range which is specific for the material. A too high temperature would completely melt the particles and cause other undesired effects, for example thermionic emission, while a too low temperature would not be sufficient to reshape the particle. The temperature needed is roughly half of the bulk melting temperature for the metal particles [19] but is challenging to estimate and is often determined through experimental methods.

Directly after the evaporation of the material, the atoms are ionized due to thermally emitted electrons and broken bonds caused by the high temperature in the furnace. Hence there will be a broad charge distribution for the aerosol particles, which renders them challenging to characterize. This problem is tackled by evenly charging the aerosol through a process called diffusion charging. The basic mechanism of this technique is to have the particles collide with ions in a controlled environment.

Diffusion can be divided in two main groups: unipolar and bipolar. As the name suggests, unipolar chargers only make use of ions with one polarity, while bipolar utilize both. The charger used in this thesis is of the latter type and is based on the radioactive decay of ^{63}Ni. The $\beta-$ decay fills the charger with bipolar ions which upon collision with the aerosol, deposit their charge. The resulting charge distribution for the nanoparticles, after enough time in the charger, will follow the Boltzmann distribution around zero [20]. The aerosol is therefore charge neutralized. The amount of particles with positive or negative charges will

increase with their diameter. However, in the regime in which we operate ($\sim$ 80 nm), the amount of doubly and triply charged particles is negligible.

2.1.2 Size selection

The aerosol particles created through the evaporation/condensation technique have a very broad size distribution. However, since they will act as seed for the nanowire growth process, we need to select specifically sized nanoparticles. For this purpose we adopt a Differential Mobility Analyzer (DMA) [21]. DMAs are based on exploiting the size-dependent electrical mobility that particles have in a gas. There are several geometries for DMAs; a slightly simplified version of the one utilized in this thesis is depicted in figure 3.

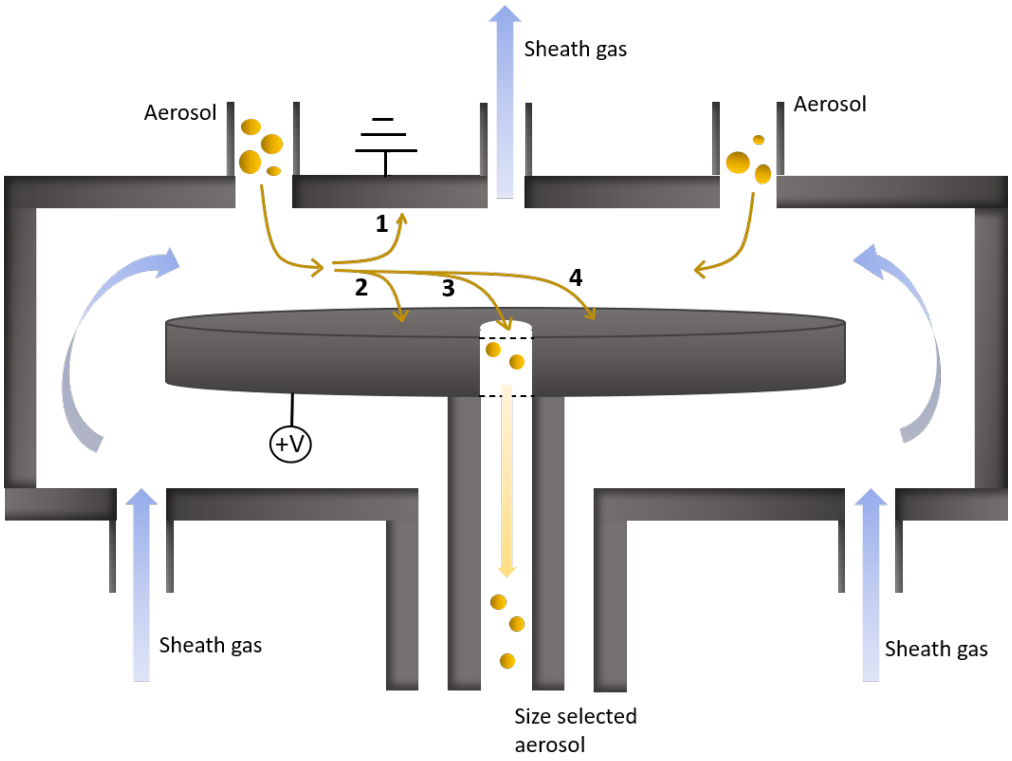

Figure 3: Cross section of the radial DMA in the Aerotaxy tool. Four different paths the aerosol particles may take are depicted: 1) positively charged particles, 2) particles with smaller than desired size, 3) particles with the desired size and 4) particles with larger than desired size.

This device consists of a disk shaped inner electrode, connected to a positive voltage source (0-10 kV) placed inside a grounded cylindrical chamber. The sheath gas is introduced from inlets placed on the bottom side of the device while the aerosol ones are placed on the top plate as shown in figure 3.

The sheath gas meets the aerosol between the two electrodes and forces the particles towards an inlet situated in the center of the inner disk. However, the mobility of the particles is strongly affected by their size, and differently sized particles will therefore take different paths. Positively charged particles will be repelled by the positive inner disk (following path

1 in figure 3), never reaching the outlet. Negatively charged particles are instead attracted by the inner disk, and their trajectory can be predicted from their diameter, the sheath gas flow and the voltage applied to the disk. Since the sheath gas flow is kept constant, we can control the trajectory of a specifically sized particle with the applied potential, allowing for size selection.

The accuracy of the DMA is limited by Brownian motion of small particles. This is most easily noticed from of the transfer function, which indicates the probability for a particle with a specific diameter to pass through the DMA. Ideally, this function should not have a width however, due to Brownian motion (and other effects caused by the gas flows), this is not the case allowing a small range of particles through the DMA. This factor is more evident for smaller particles. For the purpose of this thesis, this does not pose a problem since we do not require such accuracy. Generally, size selected particles can vary with up to ten nanometers in diameter.

2.2 Epitaxy

After size selection, the aerosol is directed into the aerotaxy section of the setup, where the actual nanowire growth occurs. To understand the growth mechanism we must first introduce a few concepts and methods which are used in regular epitaxy. Growth is caused by thermodynamic effects which tend to reach an equilibrium state, i.e. reaching the minimum Gibbs free energy (G). A small change in this energy, keeping temperature and pressure constant, is defined as the chemical potential μ

$$\mu = \frac{\partial G}{\partial N}_{T,P}, \tag{3}$$

where ∂N indicates the change in number of particles. A disparity of chemical potential between two phases will favour material transport towards the phase with the lowest potential. We can consider a vapor and a solid phase with respective chemical potential μ_v and μ_s. Assuming that $\mu_v > \mu_s$, a thermodynamically driven process will happen which will transport material from the vapor phase to the solid phase, causing crystallization. By keeping a steady supply of vapor, the process continues without reaching a steady state, hence allowing for controlled growth. In reality, the growth is more complicated, with several minor processes involved, but this model gives a general understanding of the basic process.

Generally, growth occurs in the form of layers, creating step edges for each newly deposited atomic layer. There are three main mechanisms with which this can take place: island growth, step flow growth and step bunching growth [22]. The main variable which dictates the predominant growth mechanism is the diffusion length for the atoms upon deposition. Ideally, for the growth of planes, the deposition of new atoms is confined to the step edges (step-flow growth), allowing for a homogeneous advancement of the step creating a well structured crystal lattice with scarce defects. In the case of step-bunching several minor steps might bunch together forming a higher steps, hence not completing the prior layer, leading to an unstructured lattice. For shorter diffusion lengths, atoms might not reach the step edge and instead form islands which grow when supplied with additional material (island growth). This growth mechanism is undesired due to the numerous defects formed at the interface between the islands.

2.2.1 Vapor–Liquid–Solid growth

The Vapor–Liquid–Solid (VLS) mechanism is frequently used for the growth of nanostructures [10, 11, 12]. The first reports of this method focused on the growth of so-called whiskers, which are the predecessors of nanowires. The growth mechanism is displayed in figure 4. A liquid alloy droplet is placed on a substrate and acts as a catalyst for the chemical process. For this to happen the chemical potential for the liquid droplet must follow the expression

$$\mu_v > \mu_l > \mu_s, \tag{4}$$

which allows mass transport from the vapor phase, into the liquid phase and lastly crystallization.

In paper [10], which is one of the earliest reports of VLS, Si whiskers are grown using a Au catalytic particle. The liquid particle is placed on a (111) Si substrate and alloyed with Si. The precursor ($SiCl_4$) is then introduced along with nitrogen, which acts mainly as a carrier gas. The Si atoms in the precursor get absorbed by the alloy either directly from the gas phase or by surface migration on the substrate. In the latter case the atoms first get deposited on the substrate and then "migrate" towards the catalytic particle. This will cause a supersaturation of Si in the alloy forcing future Si particles, which are still attracted by the alloy, to precipitate and crystallize. Hence a silicon whisker, with direction [111], is created underneath the alloy particle. The direction of the crystal is dictated by the direction of the substrate and the preferred growth direction.

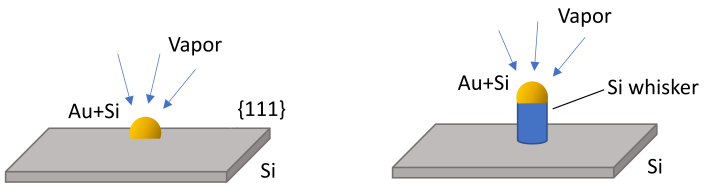

Figure 4: Basic mechanism of VLS growth.

2.2.2 Metalorganic Vapor Phase Epitaxy

One of the most utilized fabrication techniques for nanostructures is Metalorganic Vapor Phase Epitaxy (MOVPE). This process relies on pyrolytic reactions and is defined by the use of metalorganic precursors. In MOVPE, a semiconductor substrate is placed inside a hot reactor and supplied with precursors. The precursors will react on the substrate, causing epitaxial growth. The growth will be affected by the precursor ratio and it is therefore essential to carefully control the precursor flows. Ideally, the precursors should be confined to react exclusively on the surface of the substrate. This is however not the case, since reactions can take place in the gas phase, causing nucleation events in the gas which then react with the surface upon deposition. The combination of surface and gas phase reactions results in a non-trivial overall reaction [23]. Several combinations of precursors can be used, for the growth of GaAs (group III-V) we make use of group III trimethylgallium (TMG), and group V arsine (AsH_3). The total reaction is the following

$$Ga(CH_3)_3 + AsH_3 \longrightarrow GaAs + 3CH_4.$$

Dopants can be introduced in vapor form. For a III-V compound, for p-type dopants, Zn can be introduced using diethylzinc $Zn(C_2H_5)_2$ while n-type, for example Si, can be introduced with silane SiH_4. An illustration of the MOVPE fabrication technique is displayed in figure 5.

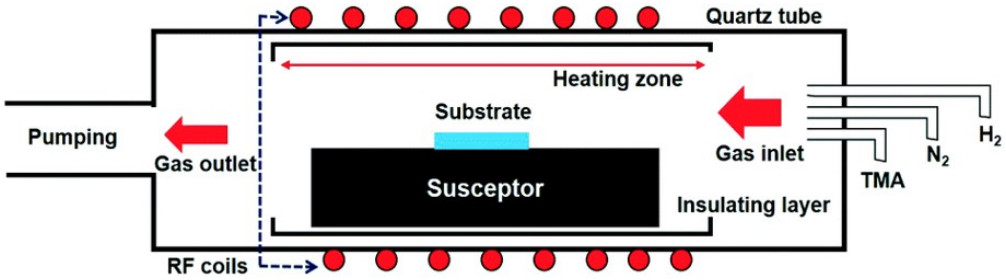

Figure 5: Illustration of the MOVPE technique. [24]

2.2.3 Self catalyzed growth

Gold seed particles, which are generally used in VLS, have the potential to introduce impurities in the nanowire's crystalline structure, therefore impacting some of its opto-electronic properties [25, 26]. With Ga as a seed particle, such impurities are avoided due to the seed particle itself contributing to the growth of GaAs nanowires. A simple schematic of self-catalysed growth is depicted in figure 6. The seed particle is consumed by growth reducing in size during the process. Introducing only the AsH_3 precursor would cause the particle to quickly be depleted, halting growth. However by introducing supplemental Ga, in the form of TMG, the particle can pursue growth until reaching depletion. Therefore, to achieve a stable step flow growth, a balance between the consumed Ga (affected by temperature, AsH_3 flow and particle diameter) and supplemented TMG must be attained.

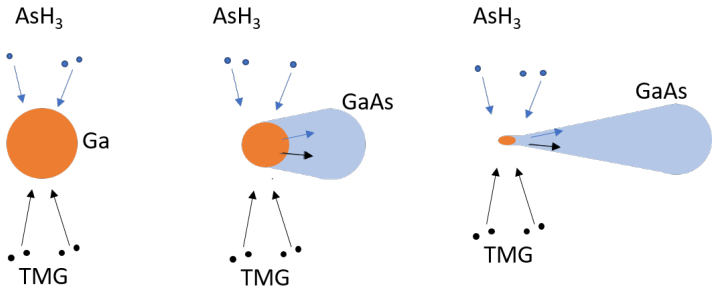

Figure 6: Schematic of the growth mechanism for self catalyzed growth. In this case the TMG flow is not sufficiently high to prevent shrinking of the seed particle during growth.

2.3 Setup

A schematic of the complete setup is shown in figure 7 [27]. Nitrogen is introduced as a carrier gas in the High Temperature (HT) furnace, in the bubbler and in the group V inlet. A sheath gas is introduced in the DMA, as explained in section 2.1.2, as well as in the aerotaxy reactor,

where it is used to avoid material deposition on the inner walls. The sheath gas is introduced with a larger flux than the carrier gas for the aerosol with the intent of avoiding mixing. The carrier gas is introduced in the furnace with a flow of 1.5 l/min while the sheath gas has a flow of 4 l/min. The group III precursor is introduced first in the alloying zone of the reactor, and then again in the growth zone to allow for a steady saturation of the seed particle. The group V precursor is introduced only in the growth zone.

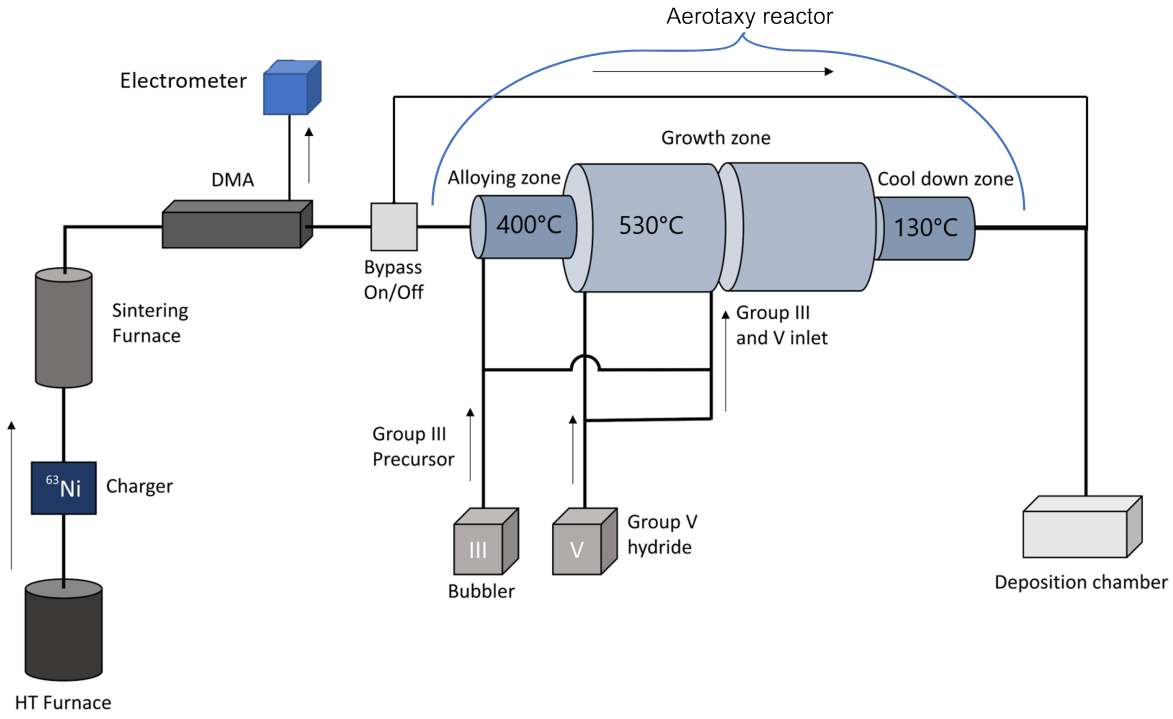

Figure 7: A schematic of the aerotaxy setup.

In figure 7 a bypass is placed after the DMA. The purpose of this is to allow for the possibility to inspect the nanoparticles directly from the aerosol section. A small aerosol flow from the DMA is directed towards an electrometer to measure the amount of created particles, which is possible due to the even charge distribution of the aerosol particles.

Pictures of the setup are displayed in figure 8.

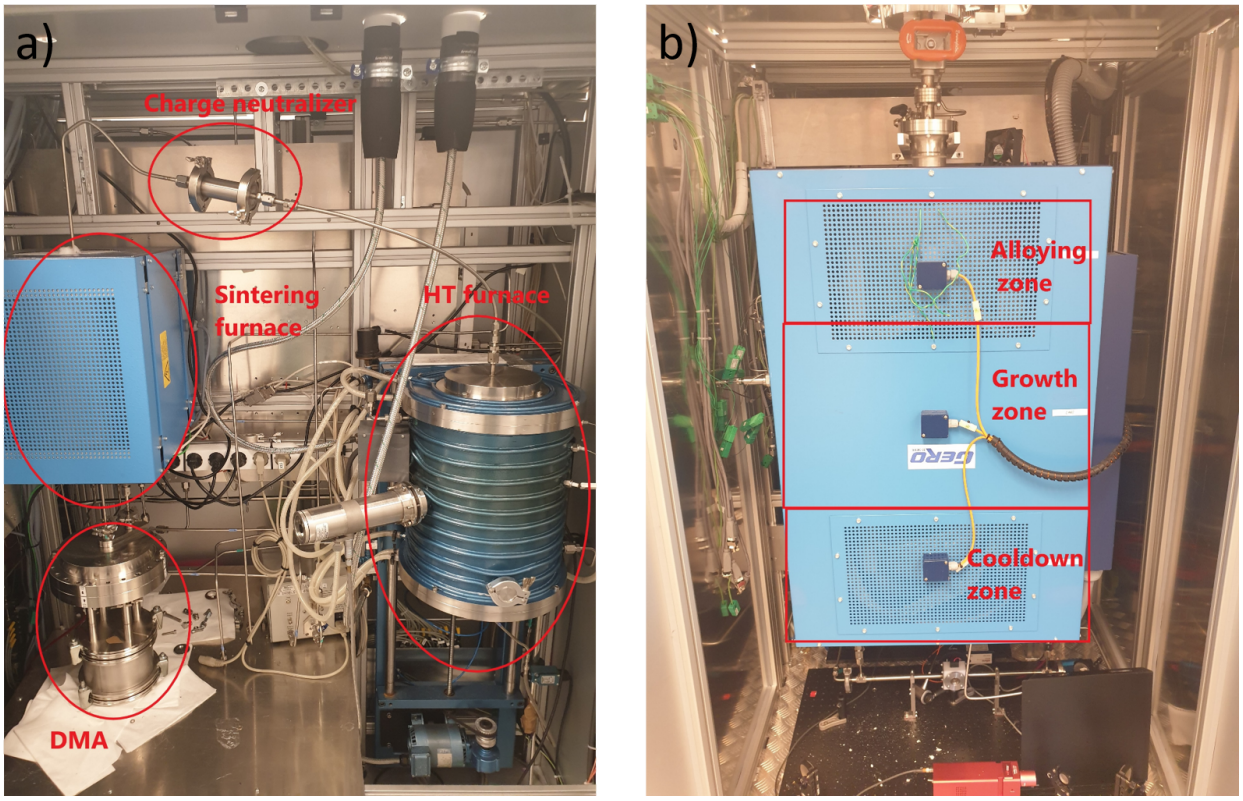

Figure 8: a) Picture of the aerosol section of the setup, b) Picture of the aerotaxy reactor.

2.3.1 Aerotaxy

The most distinct feature of aerotaxy is the epitaxial growth from an aerosol seed particle instead of a substrate [28]. The growth follows the VLS model, since a liquid nanoparticle acts as the catalyst for the reaction. We make use of MOVPE by introducing precursors in the gas phase which are then mixed in a hot flow through reactor. The liquid group III precursor resides in a bubbler which is cooled to avoid condensation in the gas lines. A carrier gas, in our case nitrogen, is pumped into the liquid thereby creating bubbles. A saturated precursor is then transported into the reactor. The precursor flow can be controlled by the carrier gas flow and the temperature of the bubbler.

The aerotaxy reactor is divided into three zones: an alloying zone, a growth zone and a cooling zone. For the growth of GaAs wires, the alloying zone is kept at 400 °C. Here the aerosol is mixed with the group III precursor (TMG). A small portion of the Ga atoms will break their bonds with the precursor and alloy with the aerosol particles. The alloy is then transported towards the growth zone. Here the second precursor, arsine, is introduced. The temperature of this zone is slightly higher (530 °C) to allow for arsine cracking and chemical reactions between precursors. The arsenic is dissolved in the seed particles which become supersaturated with both Ga and As. Following the VLS mechanism, the excess material precipitates as GaAs according to the chemical reaction explained in section 2.2.2. In the absence of a substrate, nucleation events are more challenging to achieve due to the absence of a surface on which heterogeneous nucleation can take place. A higher degree of

supersaturation is therefore required in aerotaxy due to the growth being caused exclusively by homogeneous nucleation. A constant degree of saturation is achieved with a constant flow of arsine and TMG, allowing the particle to be replenished of the precipitated material. Each nucleation event will likely take place close to the previous one, therefore quickly creating a crystal around the seed particle. Future nucleation events will then lead to epitaxial growth.

Different crystal lattices grow at different speeds, and generally, an epitaxially grown crystal assumes the direction of its slowest growth. This is most easily visualized by imaging growth on planar surface. At the outskirts, it is slowed by the surface's geometry, while in the center remains unaffected. This will quickly create a new plane in which the growth will be slower. The slowest growth direction for GaAs is [111], causing the nanowires to assume this direction.

After growth, the nanowires are transported through a cooling zone, kept at 130 °C, with the only purpose of avoiding turbulence caused by a sudden change in temperature after the growth zone. The wires are lastly transported to a deposition chamber where they are deposited on a Si wafer placed on an Electrostatic Precepitator (ESP).

2.4 Characterization

The imaging of samples at the nanometer scale requires specific microscopy techniques which go beyond optical imaging. The most commonly employed technology is electron microscopy which exploits the interaction electrons have with the sample. A beam of accelerated electrons is directed towards the sample using magnets, where the interaction with the sample produces a variety of signals which are then captured by a detector. The resolution is directly related to the wavelength of the electrons, and due to their extremely short wavelength we can achieve an excellent resolution.

There are several electron microscopy techniques, among the most popular ones are transmission electron microscopes (TEM), often used in electron diffraction mode to inspect the structure of samples, scanning electron microscope (SEM), which reveals the samples surface topography, and scanning transmission electron microscope (STEM) which is a combination of the two. The main tool employed for the morphological characterization of the samples in this thesis is the scanning electron microscope. With SEM two signals are created, backscattered electrons and secondary electrons, of which the latter is the most commonly used.

Backscattered electrons are originated by elastic collisions of electrons with the sample causing changes in their trajectory. The signal is strongly dependent on the atomic number of the specimen since a heavier atom will scatter a larger amount of electrons. Secondary electrons are instead emitted by the sample through inelastic scattering. Their emission is caused by the collision of other radiation with the sample causing electrons to be emitted. Due to their low energy, they are emitted by the surface region of the sample, a few nanometers deep. The resolution of the SEM is dependent on the amount of material the electrons interact with, decided by the electron spot size as well as the penetration depth of the electrons which is proportional to the energy of the beam. The larger the amount of material, the lesser the resolution, which generally lies between 1 and 20 nm.

3 Results

The growth of GaAs wires from Ga seed particles first requires well sintered size selected seed particles. This proved to be more challenging than expected and therefore required an own brief study which is described in the first part of this section. The wire growth is then studied through the exploration of different parameters and their effect on wire size and shape.

3.1 Ga seed particles

Gallium exists as a liquid at room temperature, therefore sintering was not believed to be necessary. However the first experiments, which utilized no sintering, revealed the formation of agglomerates instead of spherical particles. These particles are displayed in figure 9. Due to the surprising results, the Ga source material is believed to have been oxidized on the surface, hence preventing the particles to sinter into a spherical shape. However, fresh Ga presented the same behaviour, suggesting other effects. The depositions are displayed in figure 9.

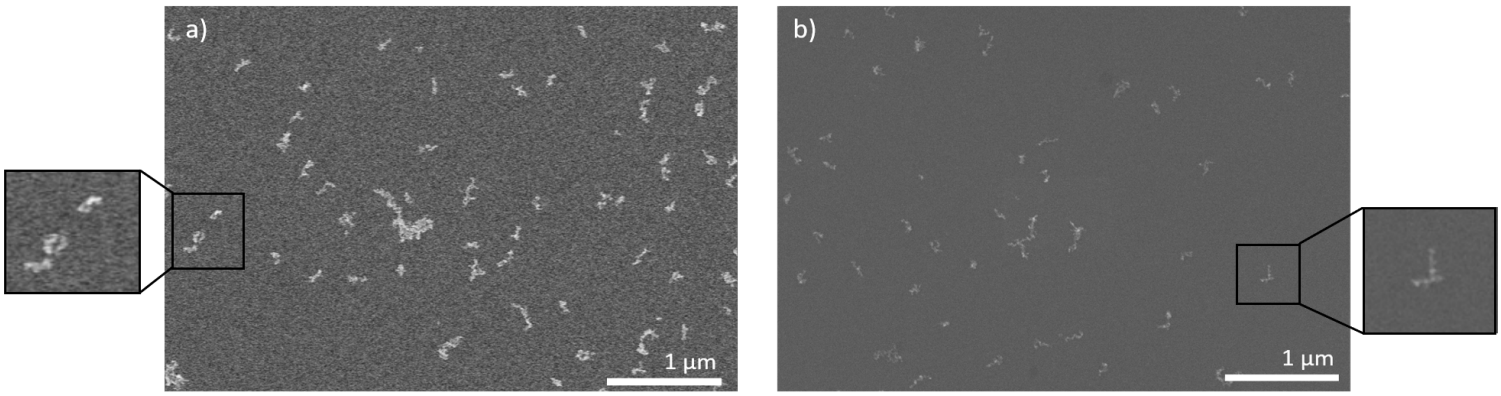

Figure 9: 80 nm unsintered Ga nanoparticles, a) aged Ga and b) new Ga.

The particles produced without sintering do not reach a satisfying quality, hence, sintering was introduced with the purpose of melting the agglomerates into spherical particles. A series of sintering temperatures was performed, ranging from 350 °C to 500 °C in steps of 50 °C. The results are displayed in figure 10.

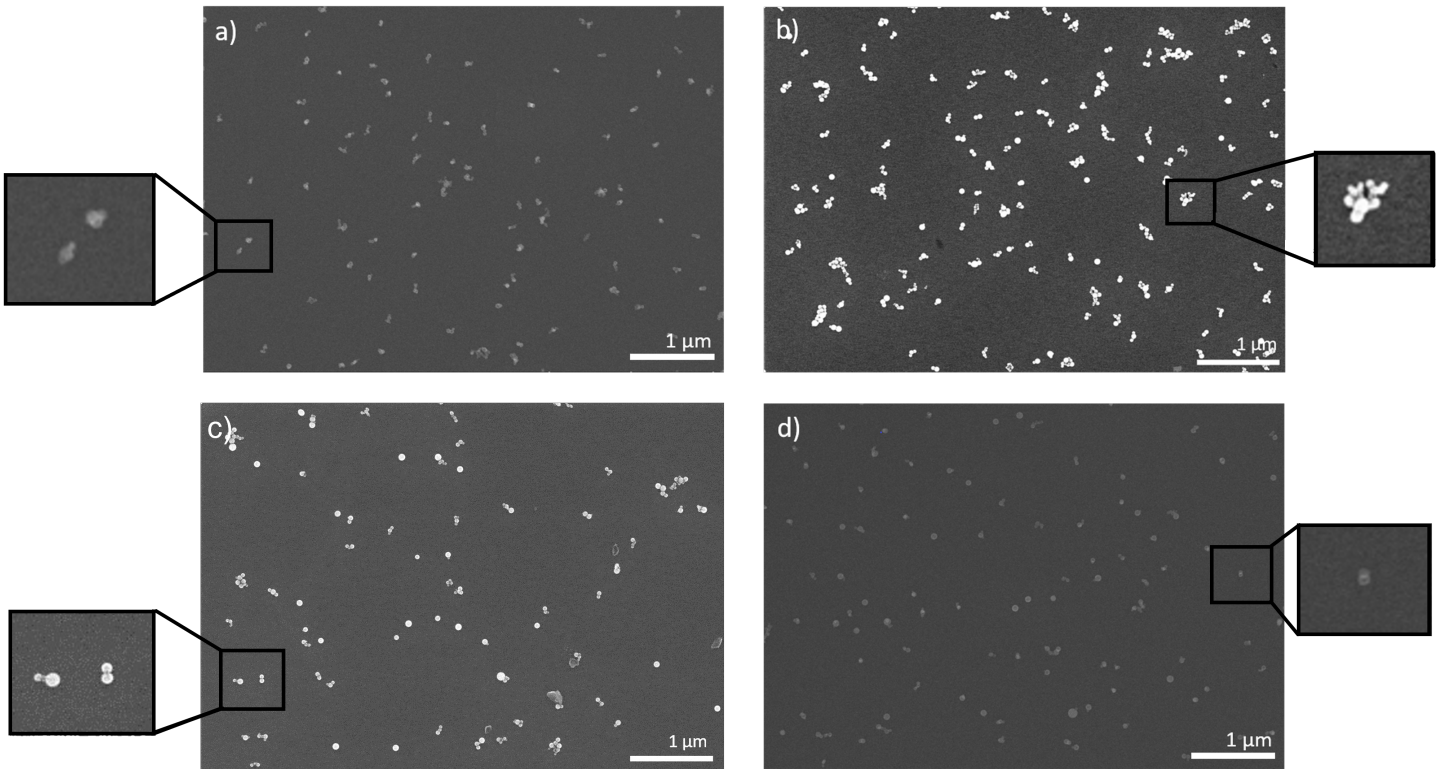

Figure 10: 80 nm Ga nanoparticle, with size set by the DMA, for a) 350 °C , b) 400 °C , c) 450 °C and d) 500 °C.

The percentage of spherical particles for the different sintering temperatures is plotted in figure 11. (This was calculated by counting the amount of spherical particles, without agglomeration, in comparison to the total amount of particles in the image). The highest percentage is found for 450 °C and is therefore the sintering temperature which was chosen for future experiments. At higher temperatures the quality decreased which is most likely due to further oxidation facilitated by the higher temperature and by small oxygen leaks in the tool.

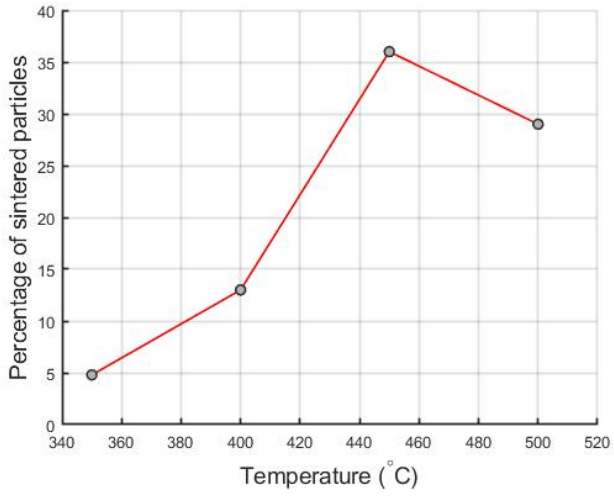

Figure 11: Fraction of Ga particles that have been fully sintered.

3.2 GaAs nanoparticles

The sintering experiments were performed bypassing the aerotaxy reactor, only focusing on the particles from the aerosol section of the tool. To investigate how the reactor may affect the seed particles, experiments were conducted flowing the aerosol through the reactor in the absence of precursors. The reactor temperatures are the ones intended for the nanowire growth, 400 °C for the alloying zone, 530 °C for the growth zone and 130 °C for the cooldown zone. The deposition is displayed in figure 12.

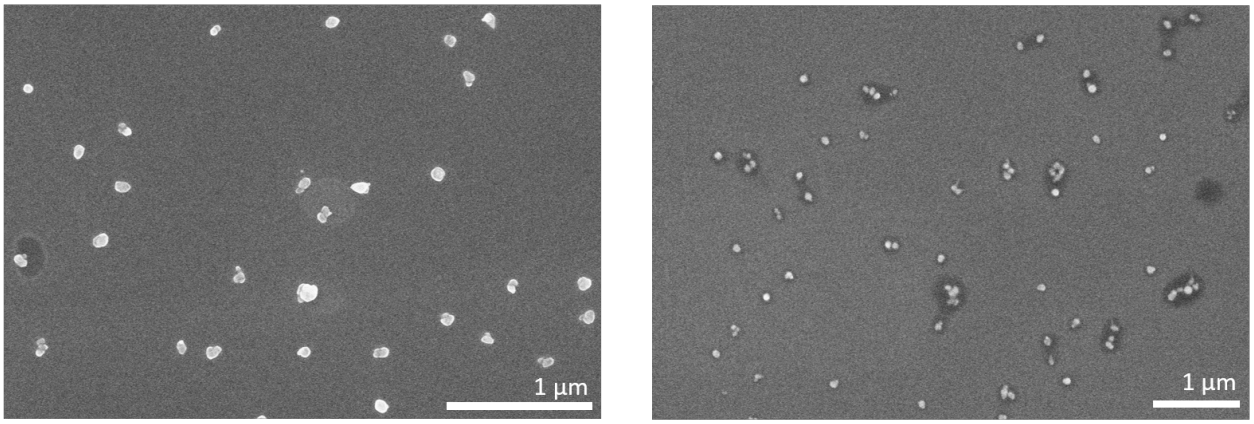

Figure 12: Ga particles, with partial conversion to GaAs, after passing through the reactor at 530 °C.

The mean diameter for the particles is 87 nm which is slightly larger than 80 nm after the DMA. The increased size is likely caused by a partial conversion to GaAs due to residual arsenic on the inside the reactor which is released at the high temperature.

GaAs nanoparticle were then grown by introducing arsine without any TMG. Three different arsine flows were tested, 0.6 sccm (standard cubic centimeters), 1.2 sccm and 2 sccm. The depositions are displayed in figure 13.

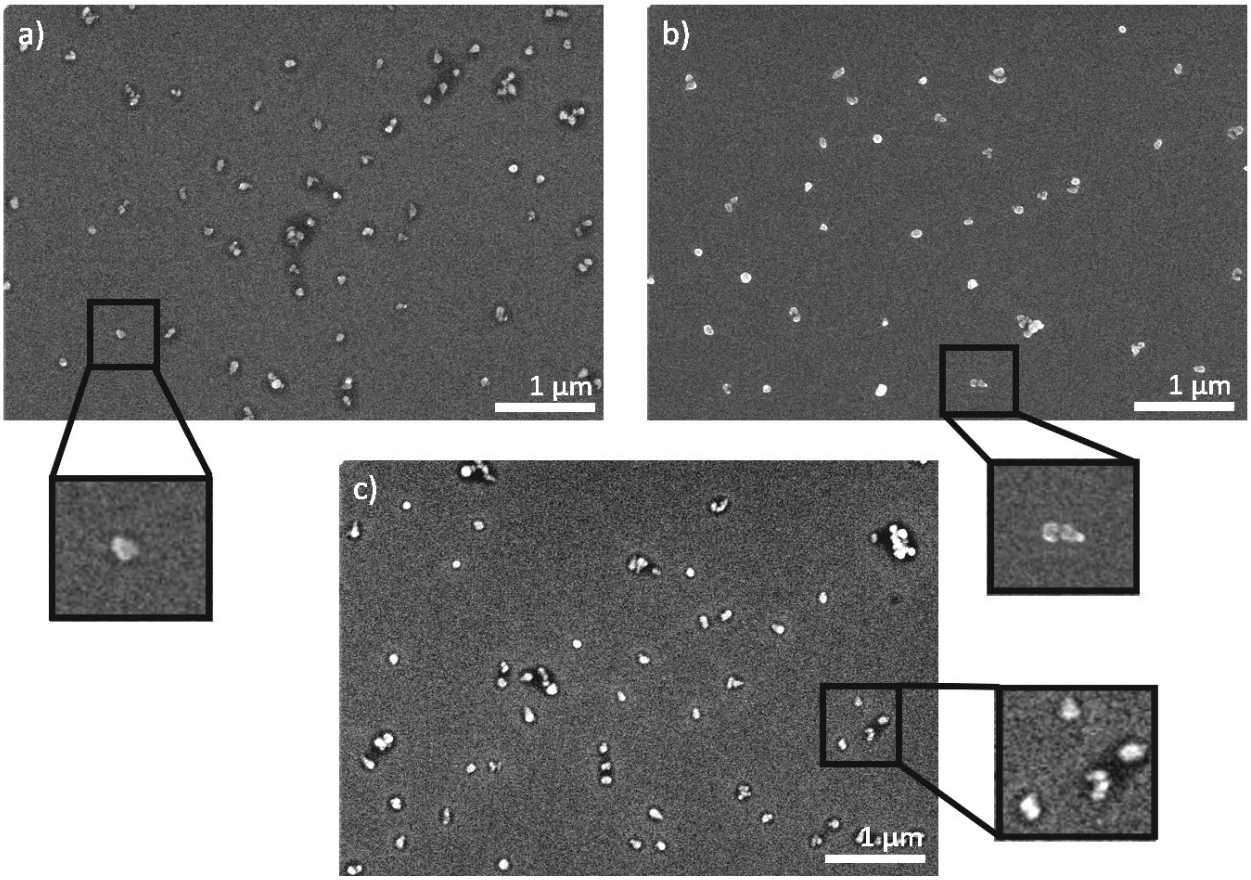

Figure 13: GaAs nanoparticles grown by aerotaxy with arsine flows of a) 0.6 sccm with relative size 1.25, b) 1.2 sccm with relative size 1.65 and c) 2.0 sccm with relative size 1.71.

The relative size of the particles was calculated by comparing their size to the one of the particles flown through the reactor in the absence of precursors. The measurements were performed on twenty particles using an image processing software called ImageJ. The particle size increased with the arsine flow due to more As contributing towards growth. Most noticeable is the shape of the particles for the 2.0 sccm flow which, instead of being spherical, presented an elongated shape which indicates a preferred growth direction. The elongation of particles during conversion has been reported in a previous paper on conversion of In particles to InP [28].

3.3 GaAs nanowires

The main goal of this thesis is to grow GaAs nanowires from the Ga seed particles, and due to the novel material used for the seed particle, this is considered an explorative study. Hence, all the results shown in this section can only be compared to the gold seed counterpart.

In aerotaxy, the wire growth is affected by different parameters e.g. precursor flows, seed particle diameter and temperature of the reactor. The exploration of these parameters and their effect on growth is reported in this section.

3.3.1 80 nm seed particles

In the case of gold particles, the most commonly used parameters at which the wires are grown are 80 nm seed particles, 2.32 sccm TMG, 2.07 sccm AsH_3 and a temperature of 530 °C. Hence, the first attempt at wires growth was conducted adopting these parameters. The results are shown in figure 14.

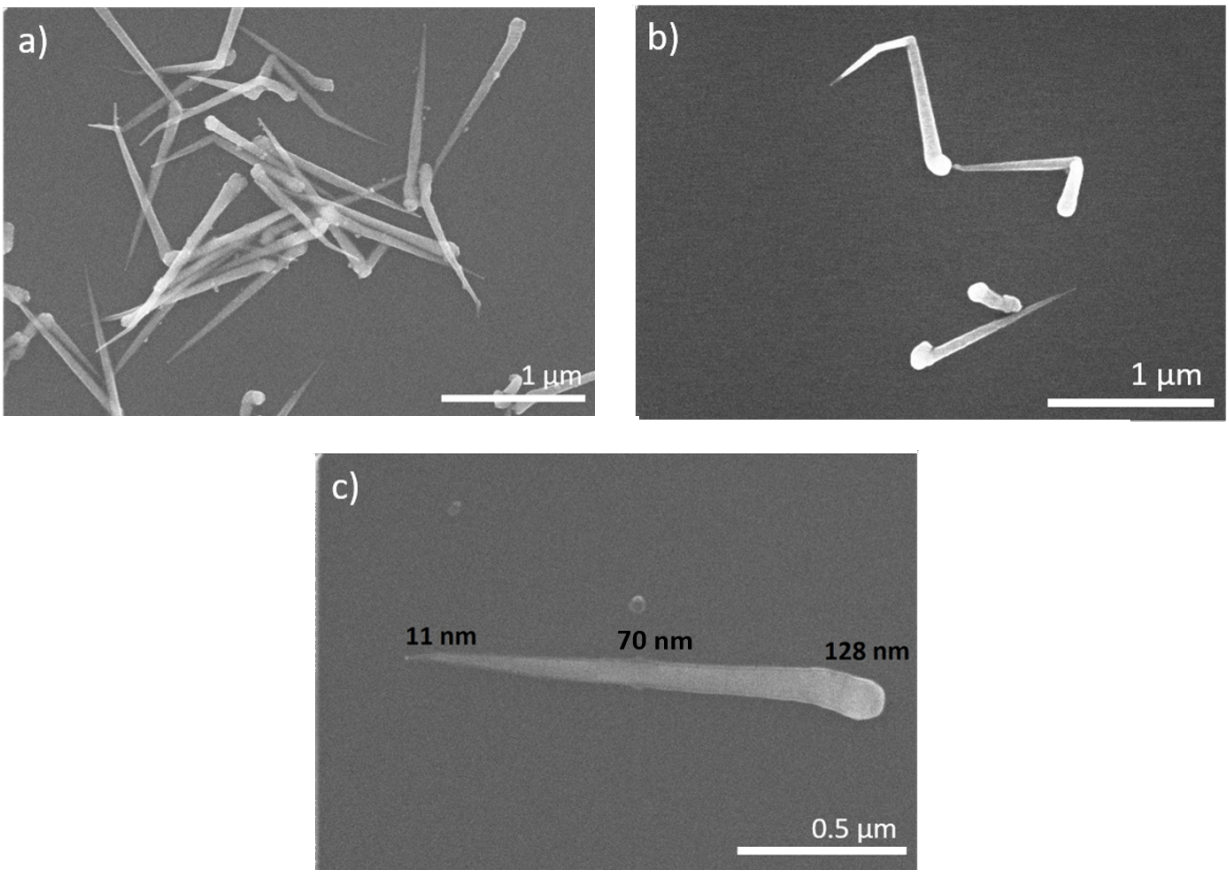

Figure 14: GaAs nanowires grown from Ga seed particles with 2.32 sccm TMG and 2.07 sccm AsH_3.

The length and thickness of the nanowires under these growth conditions with their corresponding standard deviation is 1.285 ± 0.135 μm and 0.065 ± 0.006 μm respectively. The measurements were performed on twenty nanowires and the thickness was measured as the diameter of the nanowires in their midpoint. Only a few free standing wires were found due to their tendency to agglomerate during deposition as shown in figure 14 a. Parasitic particles are found to be present on the wires as well as the substrate. These are caused by nucleation events of the precursors in the reactor forming particles which attach to the wires, and are therefore not contributing to epitaxial growth.

Images of single wires reveal smooth edges indicating a well controlled growth while the seed particle is exhausted. Several wires displayed kinking, as shown in figure 14 b, at different stages of growth. This effect is caused by a shift in the growth direction at the liquid-solid interface. Kinks are most likely caused by defects in the crystal lattice during

growth, but can also be caused by a slight shift in the temperature profile. Kinking has previously been observed for gold seeded nanowires, for specific growth conditions. In figure 14 c the size of the wire at different sections is displayed. It is shown that the diameter of the particle initiating growth is far larger than the one for the particles entering the reactor indicating growth prior to the wire formation. This effect is caused by the supplemental Gallium introduced in the alloying stage which contributes to the size of the seed particles, as well as axial growth from the arsine precursor. Hence, larger amounts of Gallium should be present in this section of the wire. The smooth surface of the wire conveys a stable growth in the central section of the wire which upon seed particle depletion reduces to a minuscule particle.

Figure 15 compares gallium seeded GaAs nanowires with gold seeded GaAs nanowires. The most noticeable difference between the two is the tapered morphology for gallium seeded nanowires which is not present in the case for gold. This is due to the catalytic particle not being consumed during growth in the latter case, hence retaining its diameter. The length of the wires is impacted by the same effect, since growth may consume the seed particle prior to reaching its maximum length. Kinking is less frequent for gold particle seeded growth, which is most likely caused by the increased growth stability offered by this catalyst.

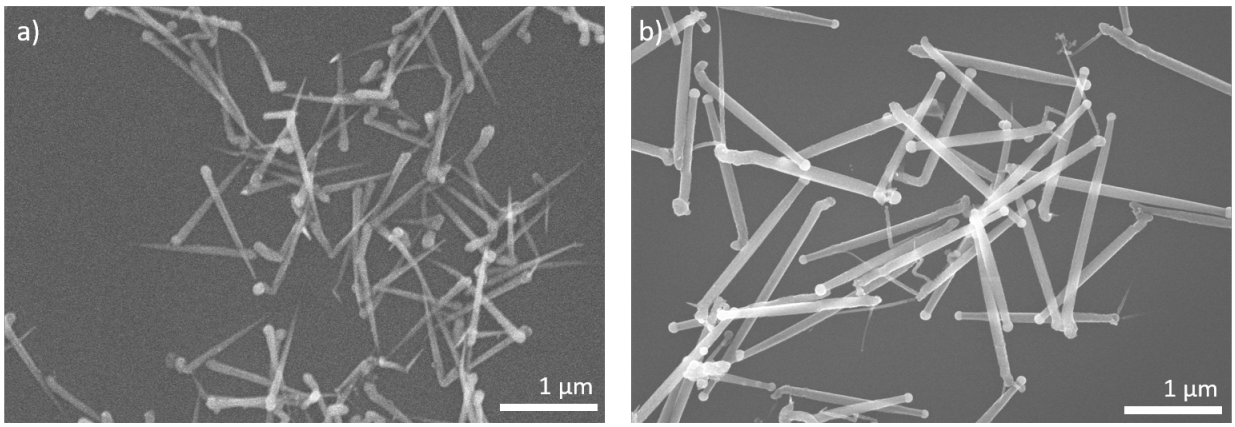

Figure 15: GaAs nanowires grown from a) 80 nm gallium seeds and b) 80 nm gold seeds with identical precursor flows and reactor temperature.

Supplemental experiments exploring different precursor flows reveal changes in the morphology of the wires. These results are displayed in figure 16. An elevated arsine flow (figure 16 a) generated a substantial increase in parasitic particles due to the higher nucleation rate of GaAs particles in the reactor, which also provides a high enough nucleation rate for a stable growth. The morphology of the nanowires is therefore not strongly impacted, in contrast to the number of wires which is heavily diminished for these growth conditions. Growth, however, appears to be heavily affected by a lower arsine flow (figure 16 b), generating rough edges suggesting unstable growth due to the absence of the arsine precursor, causing a scarcity of As therefore inhibiting growth and generating numerous defects. The wires display a thin tail towards the end, which is typically observed for low V/III ratios in other studies on gold seeded aerotaxy grown nanowires. This is caused by the seed particle being supplied with enough TMG to pursue growth, but being limited by the absence of

arsine. TMG flow variations appeared to have minor impact on the morphology of the wire, with the main difference being more prominent kinking for a scarcity of TMG (figure 16 c). An abundance of this precursor (figure 16 d) hastily replenishes the seed particle with Ga causing uneven initial growth as well as thicker wires. This growth condition generates a substantial spread in the length of the nanowires, a minority of which are longer than for other precursor flows due to the more prominent TMG flow, which inhibits the depletion of the seed particles, leading to extended growth.

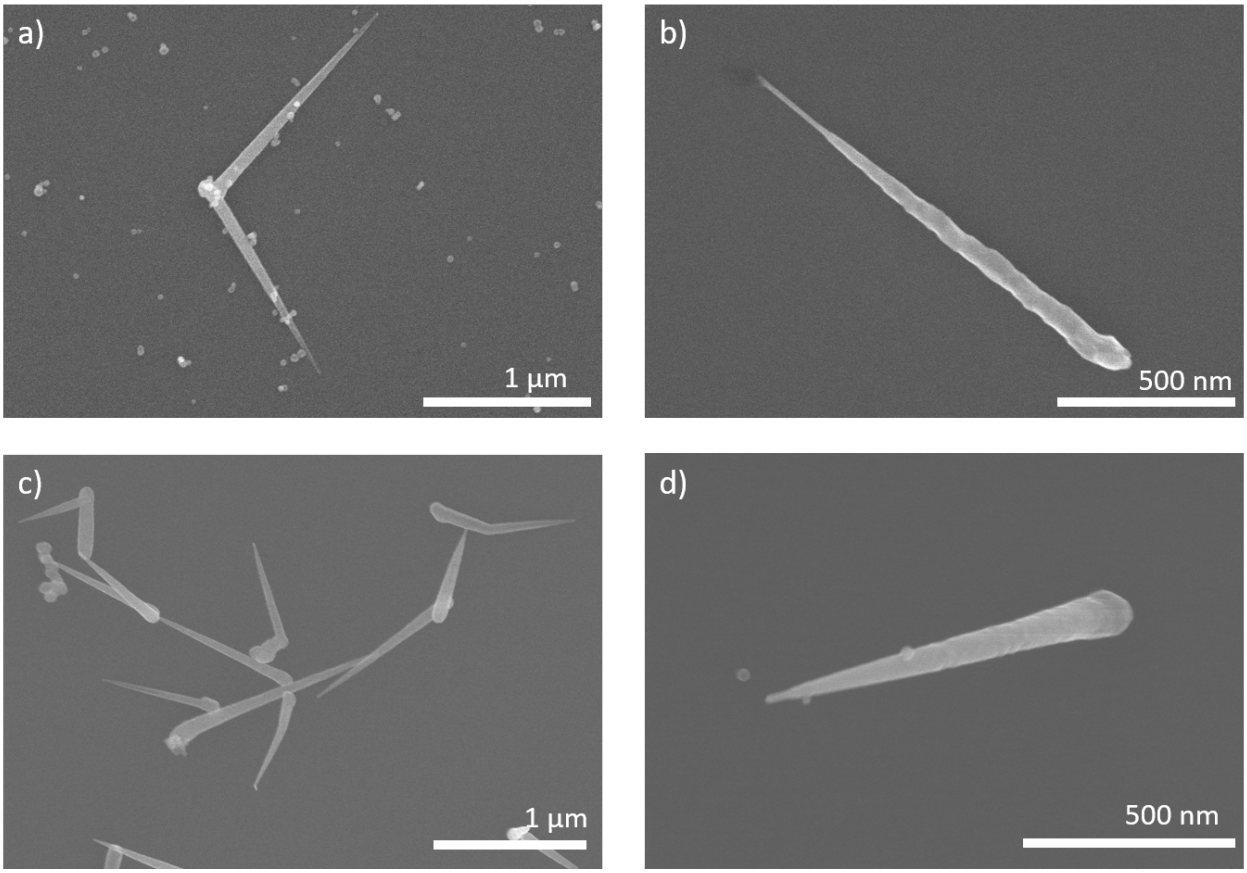

Figure 16: Nanowires grown from 80 nm seed particles with precursor flows (in sccm) of respectively a) 2.32 TMG and 3 AsH_3, b) 2.32 TMG and 1.2 AsH_3, c) 1.4 TMG and 2.07 AsH_3, d) 3.2 TMG and 2.07 AsH_3.

3.3.2 Seed particle diameter

In this section the dependence of nanowire growth on the diameter of the seed particles is explored and discussed in detail. A series of 4 experiments was conducted ranging the diameter of the seed particles from 20 nm to 80 nm. The reactor temperature and precursor flows are kept constant at 530 °C, 2.32 sccm TMG and 2.07 sccm AsH_3. Images of the 4 depositions are displayed in figure 17.

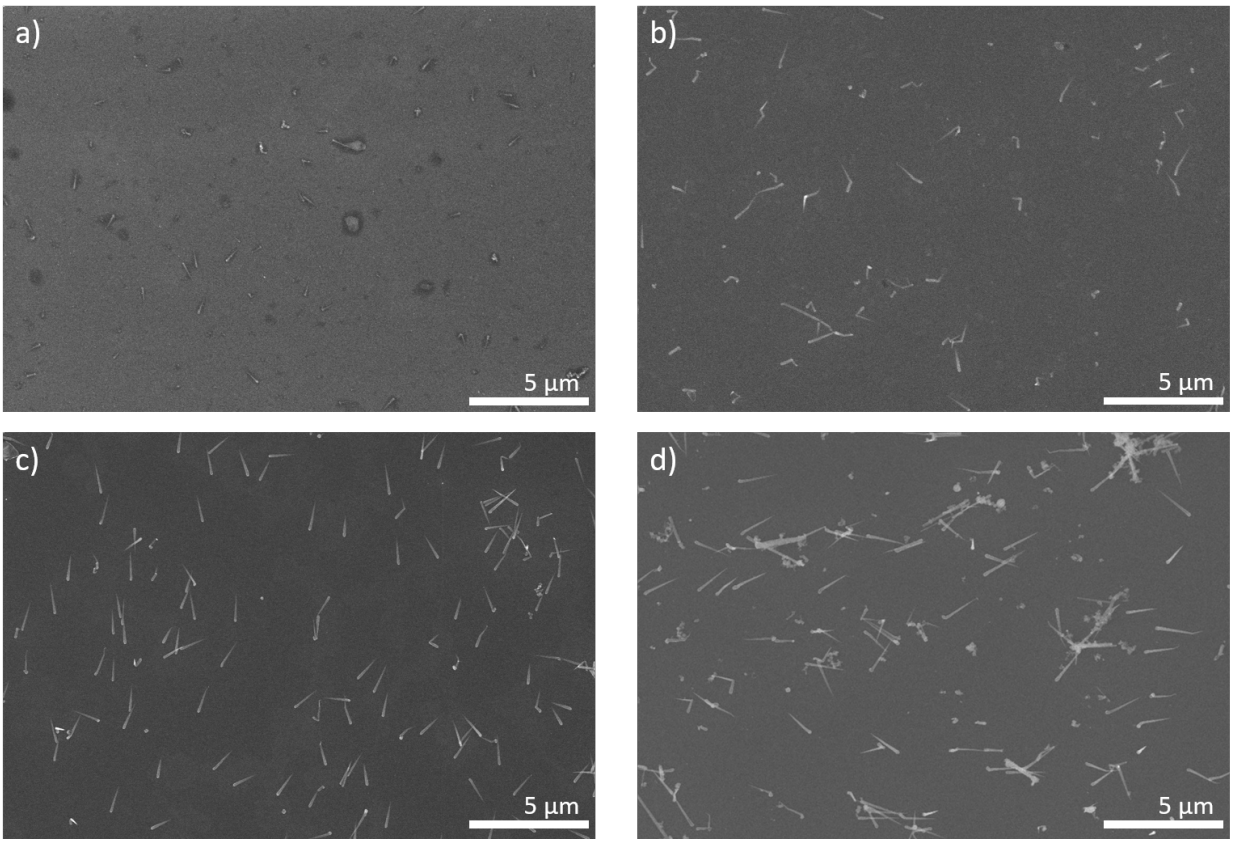

Figure 17: Depositions for nanowires grown from a) 20 nm, b) 40 nm, c) 60 nm and d) 80 nm seed particle diameters.

The length of the wires increases linearly with the seed particle diameter as displayed in figure 18. This is due to larger particles being depleted more slowly than smaller ones, allowing for longer growth time and therefore longer wires. The interplay between particle depletion due to epitaxial growth and replenishment from Ga precursor affects the morphology of the wires, as displayed in figure 17. Particles with greater diameter have an increased growth rate as well as faster replenishment due to the wider area of impingement, hence the linear relationship. The most satisfactory results are found for growth from 60 nm seed

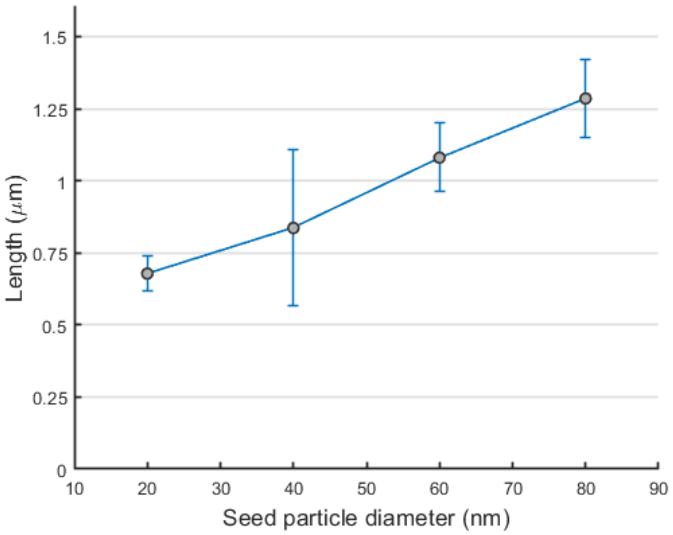

Figure 18: Length of the nanowires with corresponding standard deviation against seed particle diameter.

particles which generates uniform wires with limited kinking and scarce parasitic particles. This suggests that for these growth conditions, a balance between Ga consumption and replenishment is found, allowing for stable growth. It is noticed that kinking is prominent for nanowires grown from 40 nm seed particles, which is most likely caused by their relatively small diameter generating thinner and more fragile wires. The elevated standard deviation for wires grown from 40 nm seed particle is caused by the same effect which renders statistics unreliable.

3.3.3 Temperature

In this section, different reactor temperatures and their affect on the nanowires' morphology is explored. A series of six experiments is conducted ranging the reactor temperature from 460 °C to 560 °C in steps of 20 °C. The depositions are displayed in figure 19.

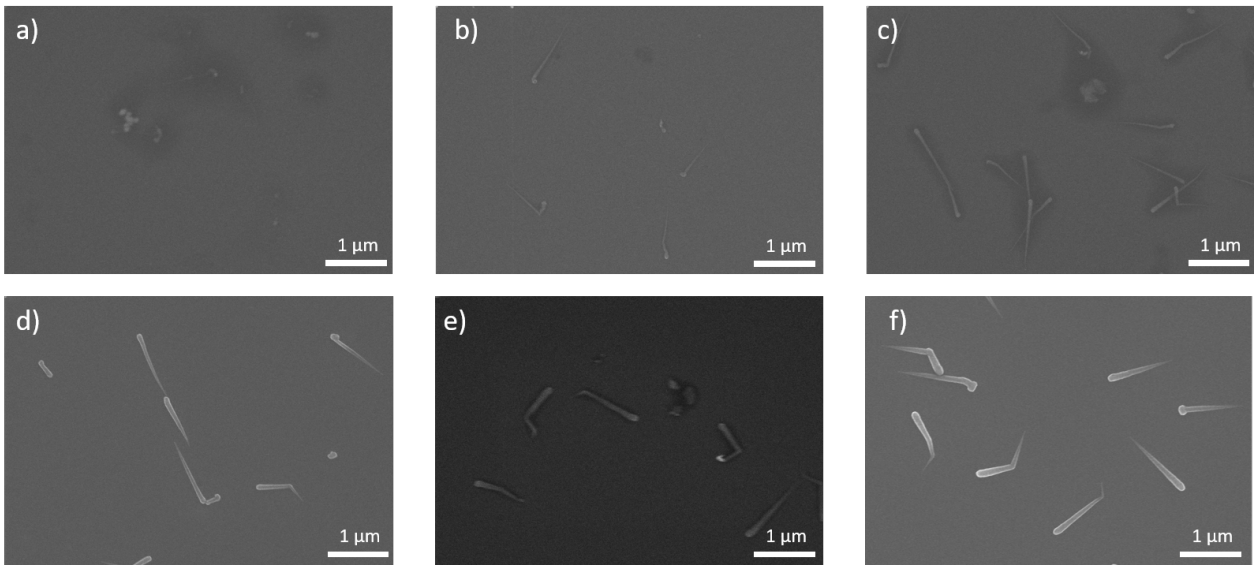

Figure 19: Depositions for nanowires grown at a) 460 °C , b) 480 °C, c) 500 °C, d) 520 °C, e) 540 °C, f) 560 °C reactor temperatures. Seed particle diameter is 60 nm with a V/III ratio of 0.89.

No growth is observed at 460 °C due to the low temperature which is unsuitable for pyrolysis and epitaxial growth. Increased temperatures present progressively thicker wires, with similar length. These parameters are plotted and displayed in figure 20. As the midpoint diameter increases with temperature the nanowires present an increasingly more tapered morphology. A comparison with similar experiments performed for gold seeded nanowires reveals a dissimilarity between the two. In the case of gold, higher temperatures are shown to increase axial growth leading to longer wires as well as more prominent tapering. This however is not found for Ga seeded wires. We see that for temperatures above 480 °C the length remains similar, suggesting a similar axial growth rate. The thickness increases in all sections of the wires indicating increased radial growth and/or a larger particle diameter before the wire growth starts. Theoretically this would cause the particle to be consumed during a longer period, creating longer wires. The results instead indicate that, while the

seed particle is larger, it is also consumed at a faster rate, generating equally long wires. The unchanged length therefore suggests that these effects are increased equally with the temperature, hence not affecting the length of the wires. Parasitic particles are found in greater extent for higher temperatures, caused by the increased nucleation rate.

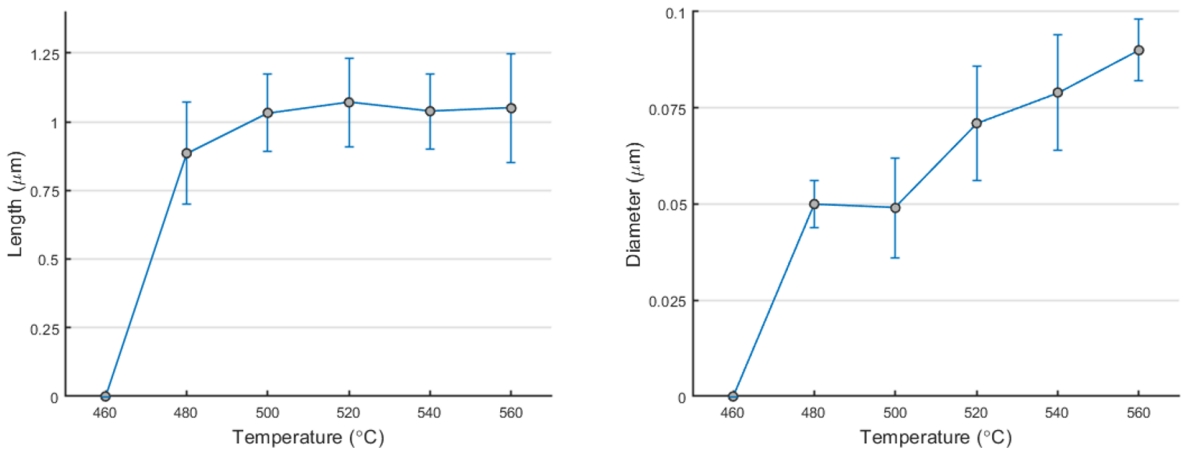

Figure 20: Nanowire length and midpoint diameter with corresponding standard deviations against reactor temperature.

A supplemental experiment was performed with the alloying stage kept at 200 °C, and compared to 400 °C alloying temperature. It was found that the growth is greatly affected by the temperature in the alloying stage due to two main effects. Firstly the seed particles absorbs less gallium due to the low temperature in this stage, hence affecting the size of the particles and amount of Ga available for growth. Secondly, the decreased temperature in the alloying stage passively affects the temperature in the growth stage, since the gas flowing through the reactor is cooler than for the standard temperatures, therefore causing a lower overall temperature which impedes growth. As observed in figure 21, only few nanowires are found on the substrate, with a significant fraction of nanoparticles absent of growth.

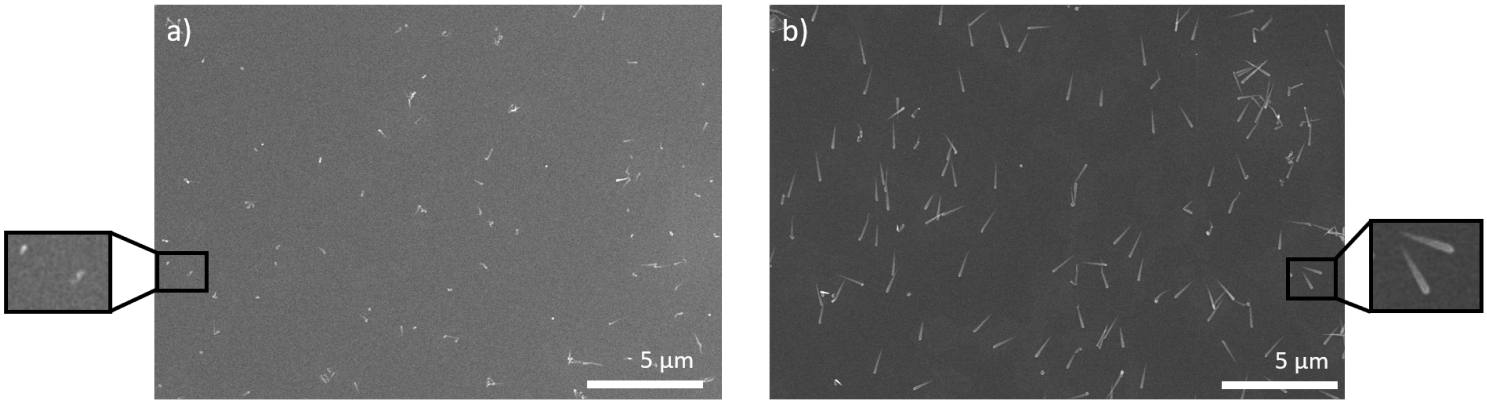

Figure 21: Depositions with a) 200 °C alloying temperature and b) 400 °C alloying temperature. 60 nm seed particles were used with a V/III precursor ratio of 0.89.

3.3.4 Parameter exploration

Concluding the experimental exploration of Ga seeded nanowire growth, two sets of 8 experiments were performed investigating precursor ratios and seed particle diameters in the proximity of the highest quality results found from previous experiments. The growth conditions chosen were those for 60 nm seed particles with precursor flows of 2.32 sccm for TMG and 2.07 AsH_3 grown at 530 °C. The first set of experiments explored growth from 50, 60 and 70 nm seed particles with different precursor ratios which was achieved using a constant TMG flow (2.32 sccm) and varying the AsH_3 flow. The depositions are displayed in figure 22. It is to be noted that the deposition for 60 nm and a V/III precursor ratio of 0.89 was not performed in this experimental series but are taken from a previous one, and can therefore result in slightly different growth conditions due to memory effects in the reactor.

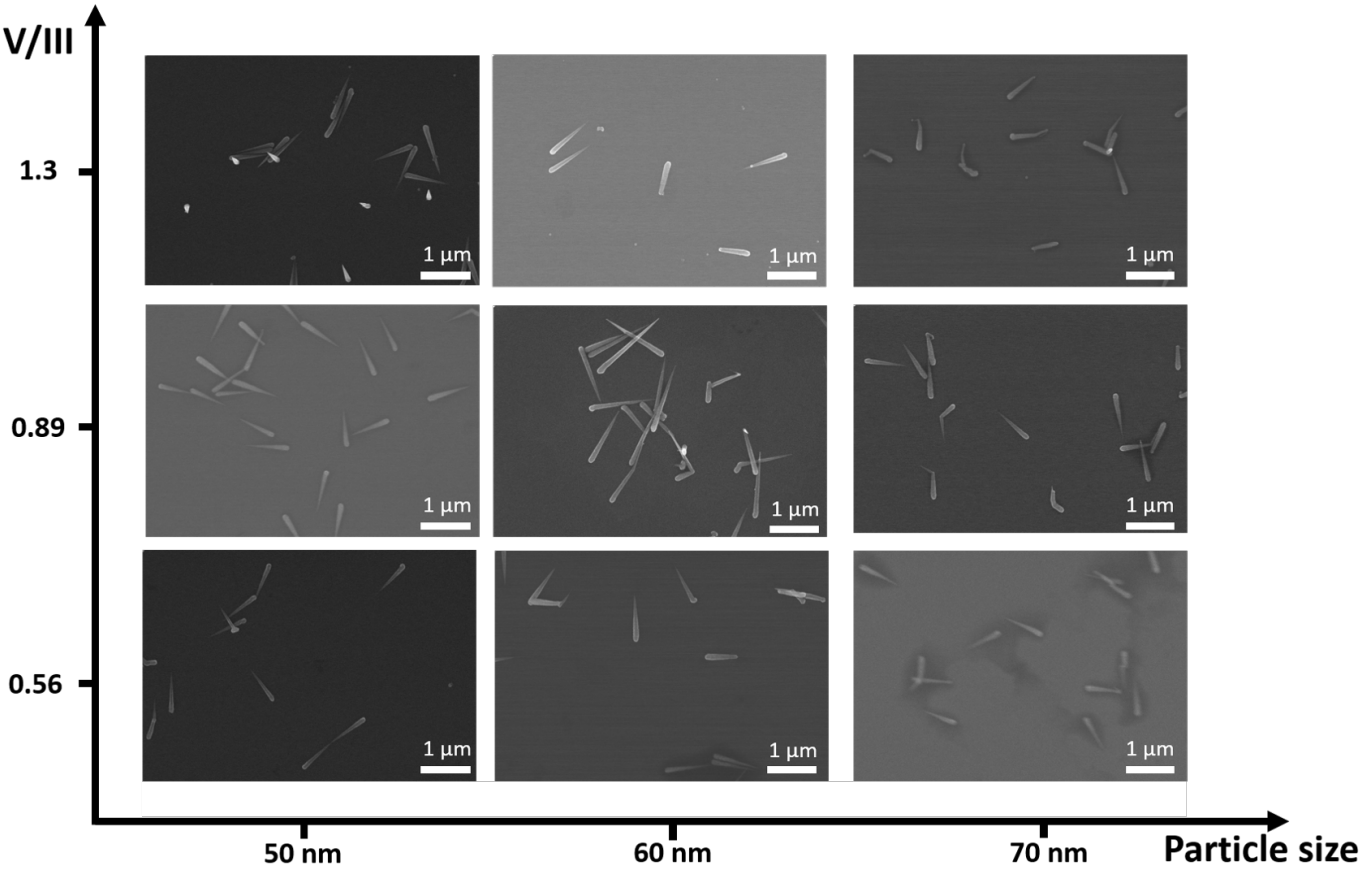

Figure 22: Depositions for different particle sizes and V/III ratios.

It was found that 50 nm particles generate uniform wires with a length of 0.82±0.08 μm using a V/III ratio of 0.89. This value slightly differs from the linear relationship found in figure 18. However upon closer inspection, the morphology of the wires varies greatly to the 40 and 60 nm cases, presenting far less kinking and sporadic growth. We can therefore assume that the growth mechanism for this parameter is different from that for its closest neighbours, resulting in more uniform wires with rare kinking and low parasitic presence.

Similarly 70 nm wires present different morphology as compared to that for 60 and 80 nm, with more prominent kinking, shorter and thicker wires. We can therefore conclude that the growth mechanism for 50 and 60 nm particles is slightly different than for larger and smaller particles. For these parameters the interplay between precursor impingement and epitaxial growth gives rise to most uniform growth, hence resulting in the highest quality wires. Statistics on the depositions displayed in figure 22 can be found in figure 23.

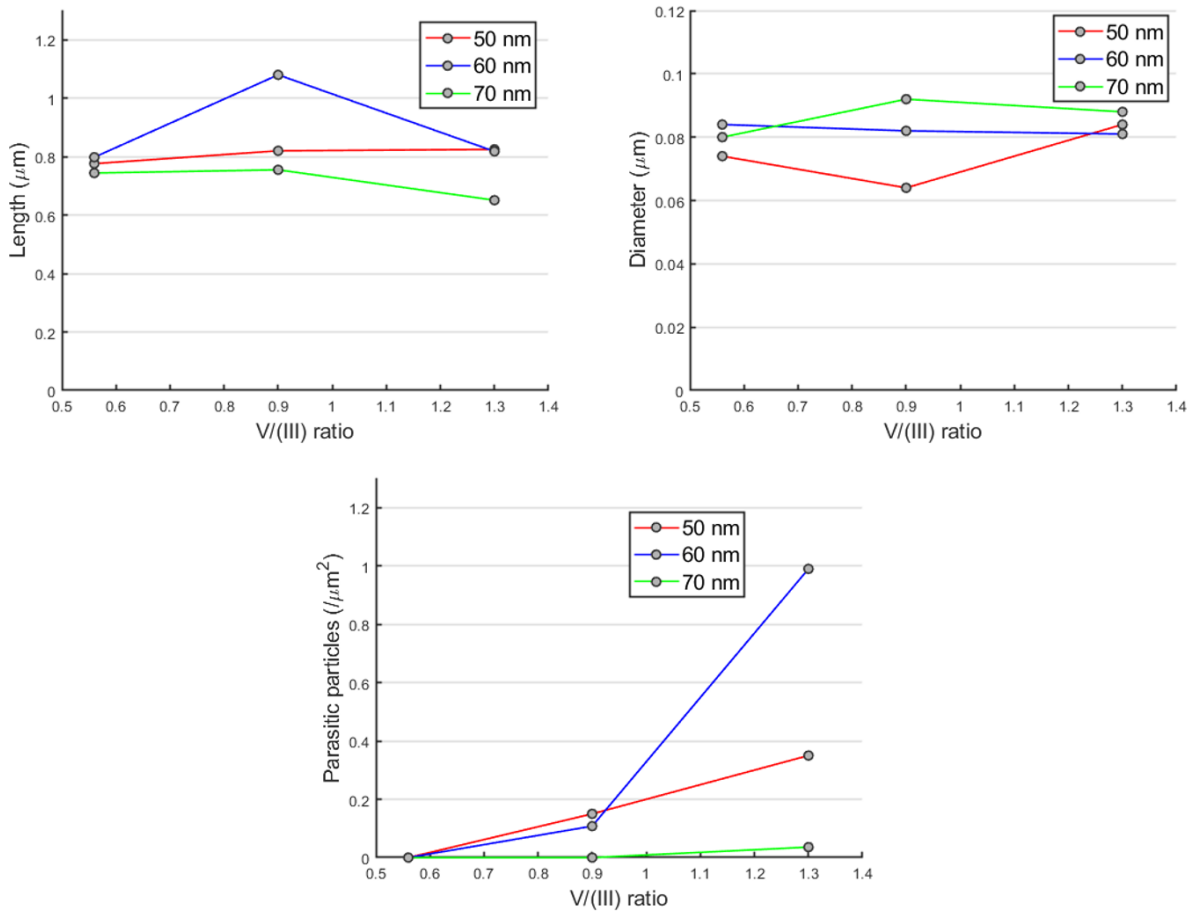

Figure 23: Length, diameter and parasitic particles for different seed particle diameters and V/III ratios.

The V/III precursor ratio has a minor affect on the wire morphology. It is found that, in general, higher V/III ratios gives rise to slightly thicker wires with increased amount of parasitic particles. The higher AsH_3 flow contributes to more sporadic growth, by hastily saturating the particle with As, hence causing more uneven wires with prominent kinking, which is best observed in the case for 70 nm seed particles. This is an explanation for the drop in wire length for high V/III precursor ratio. We can observe some similarity between the 50 and 70 nm cases, which are far shorter than the 60 nm seed particle grown in a prior experimental series. This might suggest the effect of minor memory effects, which slightly inhibit growth. Two separate sets of wires are noticed for a high V/III ratio for 50 nm particles. This indicates two different growth mechanisms for these parameters, one which

generates short and thicker wires while the other growing similar wires to other parameters.

The second set of experiments was performed to more in detail investigate different precursor flows using 60 nm seed particles. The results are displayed in figure 24.

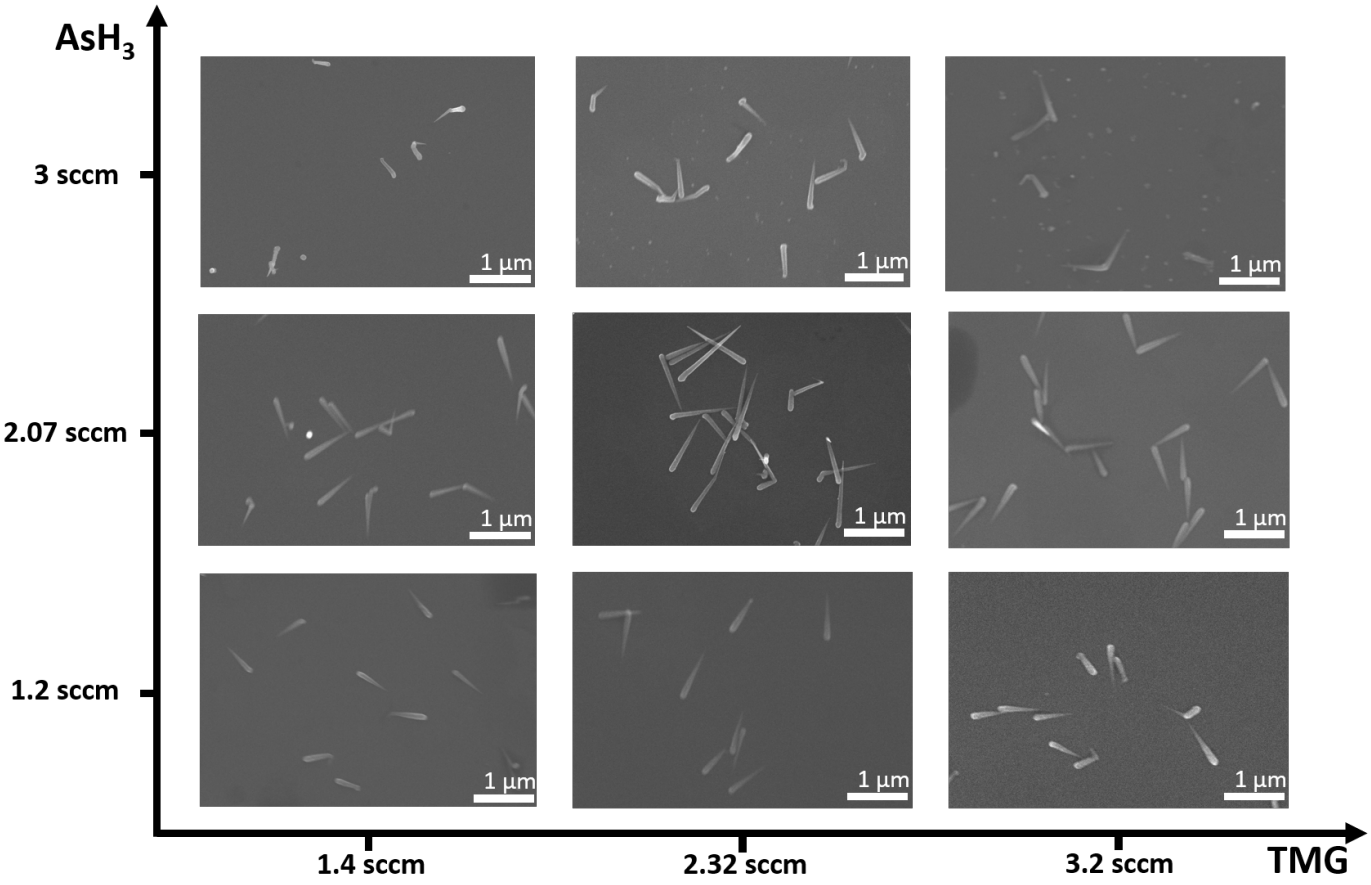

Figure 24: Depositions for different precursor flows, all wires are grown from 60 nm seed particles with a reactor temperature of 530 °C.

It can be noted that the precursor flows affect the nanowires' morphology more prominently for a few extreme cases. One example is the 3.2 sccm (TMG) - 1.2 sccm (AsH_3) deposition which results in an exaggeration of the effect noted in figure 16 b, i.e. a long tail due to the abundant TMG and scarce AsH_3. Another effect is the more prominent kinking present for a high AsH_3 flow which is caused by the swift supersaturation of the seed particle with As, which could easily lead to defects in the wire's crystal lattice and therefore slight changes in the growth direction. Parasitic particles are also found to be more noticeable for higher precursor flows, due to the more prominent nucleation which happens in this regime.

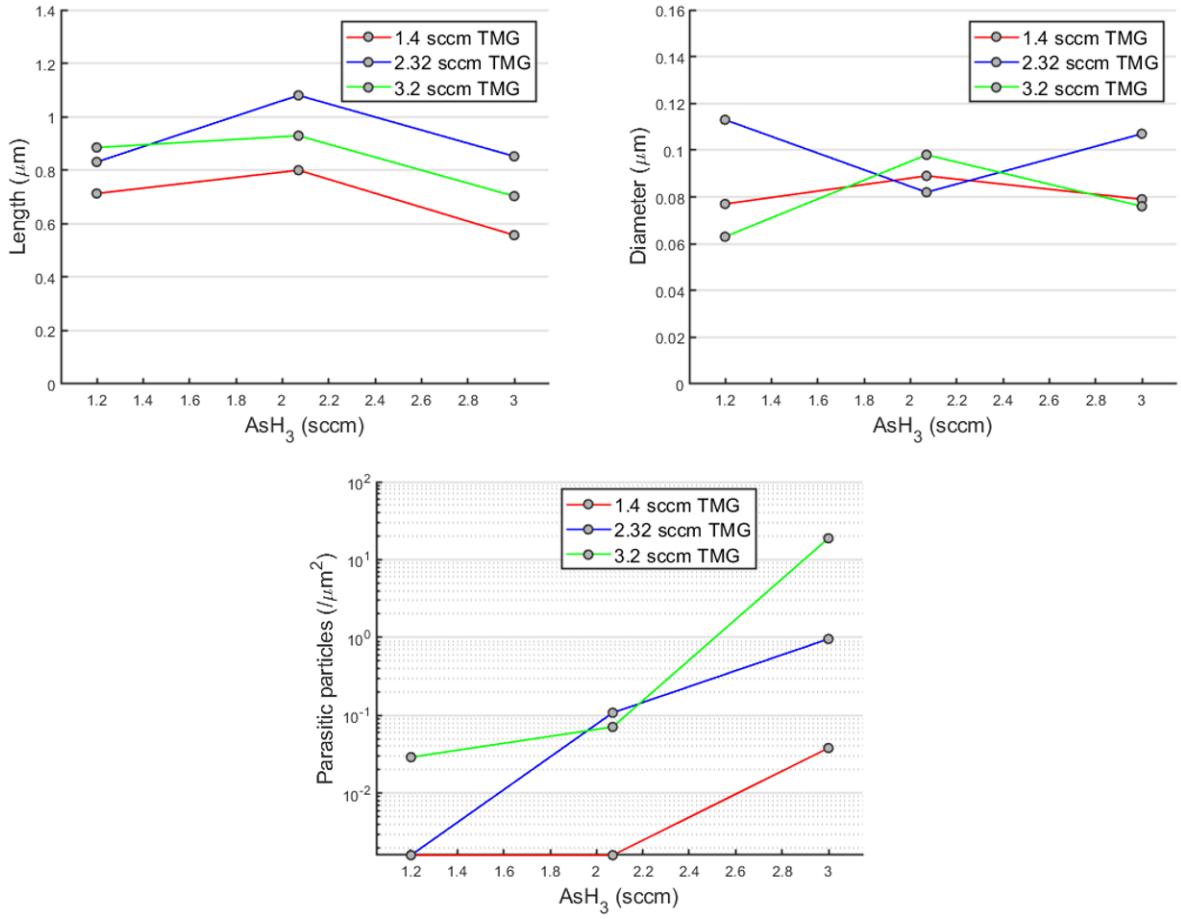

Figure 25: Length, diameter and parasitic particles for different precursor flows.

The plots display the relationship the AsH_3 flow has on the morphology of the wires for the same TMG flow. It is found that, overall, 2.32 sccm TMG gives rise to the longest wires, while 1.4 sccm the shortest. The peak in wire length is achieved for a 2.07 sccm AsH_3 flow. Lower flows slow the growth due to the absence of As, while higher flows cause more sporadic and uncontrolled growth. The rate of decrease in length is constant for all three TMG flows. The nanowires' diameter does not present any noticeable trend, it is therefore challenging to draw conclusions from this plot.

The amount of parasitic particles on the sample is found to be strongly increasing with the AsH_3 flow. The rate of increase is dependent on the TMG flow, higher flows cause more nucleation and therefore more particles.

3.4 Ga(As)P nanowires

One final experiment was performed in the attempt of growing GaP nanowires, by replacing the group V precursor from AsH_3 to PH_3. The results are displayed in figure 26. The reactor temperature was increased to 580 °C in the case of phospine due to the higher cracking temperature for this gas. The reason for the As in the nanowire is due to the residual As in the reactor.

The nanowires presented a long thin tail, which potentially indicates the supersaturation of Ga in the seed particle. Parasitic particles are also present in great extent, suggesting a high nucleation rate.

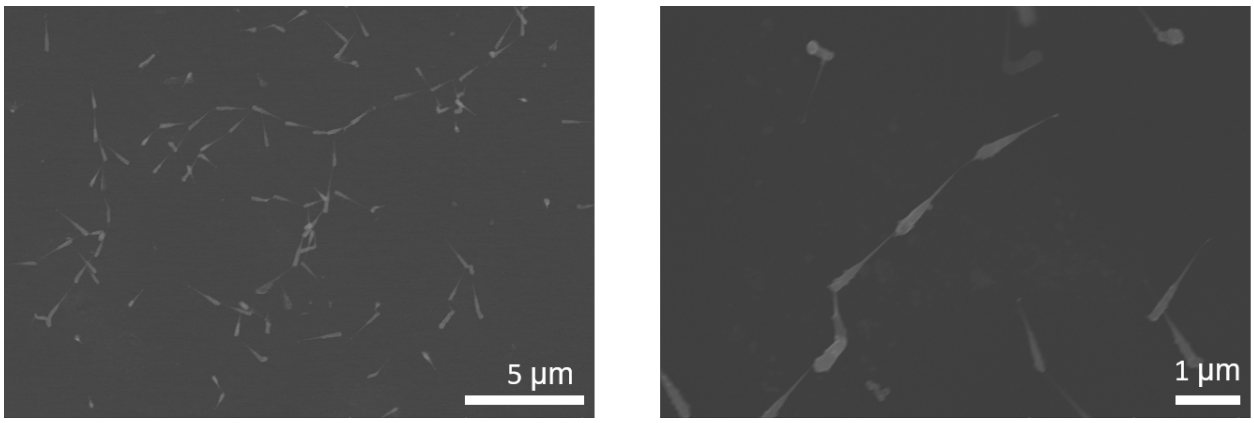

Figure 26: Ga(As)P nanowire grown from 60 nm Ga seed particles. Reactor temperature of 580 °C, 60 nm seed particles, 2.32 sccm TMG and 0.65 sccm PH_3 flows.

4 Conclusions

The goal of this work was to grow self catalysed GaAs nanowires from Ga seed particles with the aerotaxy growth method. Ga particles were more challenging to sinter than expected, most likely due to oxidation. The study was therefore proceeded using parameters which were deemed to result in the most satisfying seed particles. GaAs nanoparticles were briefly studied by supplying arsine, while withholding the TMG precursor, therefore hindering epitaxial growth. Higher precursor flows resulted in the largest particles, which also caused a more elongated shape, already suggesting a preferred growth direction.

GaAs nanowires were grown from 80 nm seed particles and through comparison with the gold seeded case, they are observed to have a far more tapered morphology. This is caused by the seed particle being consumed during growth in the self catalyzed case, hence diminishing in diameter as the growth progresses. The length of the nanowires is found to have a linear dependence on the seed particle diameter, which is due to the larger particle being more slowly depleted, hence allowing for longer growth. It is challenging to draw conclusions from results for nanowires grown 50 and 70 nm seed particle diameters due to their inconsistency with other results. This is most likely caused by memory effects and require further investigations.

Temperature was not found to have a strong effect on the length of the nanowires, but instead mainly impacted their diameter, with the thickness increasing with the temperature. This effect indicates an increase in radial growth with a constant axial component and larger initial particle.

Different precursor flows and ratios were explored, and the morphology of the resulting wires reported in several plots. Generally, higher precursor flows generate the most uneven wires with a high amount of parasitic particles due to the higher nucleation rate. The group V precursor mainly affects the morphology of the wire, causing defects and kinking. The group III precursor mainly affects the length of the wires, since it controls the amount of Ga which replenishes the seed particle, therefore controlling the rate of seed particle depletion. The highest quality nanowires in terms of uniformity, length and parasitic particle presence is found for 50 and 60 nm seed particles using a V/III precursor ratio of 0.89.

Future investigations may explore more in detail the nanowires' dependence on the seed particle diameter due to the discrepancies found in this study. Time dependence (order of experiments) is a factor which has remained untouched in this thesis, the exploration of which might offer a better overview of memory effects and growth stability. The possibility of doping is another factor which may be investigated in future experiments. Most importantly, this work proves the possibility to grow self catalysed GaAs and Ga(As)P nanowires from Ga seed particles, allowing for the development of innovative growth techniques which circumvent the necessity for Au seed particles.

References

[1] T. Oh "Analysis of Surface Current by Quantum Tunneling Effect of Thin Film Transistors with Topological Insulators" *Sci Rep* **10** 9509 (2020).

[2] Y. Xia, P. Yang, et.al. "One-Dimensional Nanostructures: Synthesis, Characterization, and Applications" *Adv. Mater.* **15** pp. 353-389 (2003).

[3] J. Hu, T. Wang Odom, C. M. Lieber "Chemistry and Physics in One Dimension: Synthesis and Properties of Nanowires and Nanotubes" *Acc. Chem. Res* **32** pp. 435–445 (1999).

[4] S. K. Sinha, K. Kumar, S. Chaudhury "Si/Ge/GaAs as channel material in nanowire-FET structures for future semiconductor devices" pp. 527-530 (2015).

[5] C. B. Zota, L. Wernersson, E. Lind "High-Performance Lateral Nanowire InGaAs MOSFETs With Improved On-Current" *IEEE Electron Device Letters* **37** pp. 1264-1267 (2016).

[6] J. Wallentin, N. Anttu, et.al. "InP Nanowire Array Solar Cells Achieving 13.8% Efficiency by Exceeding the Ray Optics Limit" **339** pp. 1057-1060 (2013).

[7] T. Fukui, M. Yoshimura, E. Nakai "Position-Controlled III–V Compound Semiconductor Nanowire Solar Cells by Selective-Area Metal–Organic Vapor Phase Epitaxy" *AMBIO* **41** 119–124 (2012).

[8] M. Fu "Electrical Properties of Indium Arsenide Nanowires and Their Field-Effect Transistors" (2018).

[9] M. Magnusson "nano.lu.se/research/nanoenergy/nanowire-photovoltaics".

[10] R. S. Wagner, W. C. Ellis "Vapor-Liquid-Solid mechanism of single crystal growth" *Appl. Phys. Lett.* **4** (1964).

[11] R. S. Wagner, C. J. Doherty "Mechanism of Branching and Kinking during VI.S Crystal Growth" **115** pp. 93 (1968).

[12] E. I. Givargizov "Fundamental aspects of VLS growth" *Journal of Crystal Growth* **31** pp. 20-30 (1975).

[13] J. L. Liu, S. J. Cai, et.al. "Growth of Si whiskers on Au/Si(111) substrate by gas source molecular beam epitaxy (MBE)" *Journal of Crystal Growth* **200** pp. 106-111 (1999).

[14] L. R. Wallenberg, B. J. Ohlsson, et.al. "Size-, shape-, and position-controlled GaAs nano-whiskers" *Applied Physics Letters* **79** pp. 3335-3337 (2001).

[15] A. M. Morales, C. M. Lieber "A laser ablation method for the synthesis of crystalline semconductor nanowires" *Science* **279** pp. 208-211 (1998).

[16] D. Boulaud, J.C. Chouard, et.al. "Experimental study of aerosol production by laser ablation" *Journal of Aerosol Science* **23** pp. 225-228 (1992).

[17] W. Mahoney, R. P. Andres "Aerosol synthesis of nanoscale clusters using atmospheric arc evaporation" *Materials Science and Engineering* **204** pp. 160-164 (1995).

[18] R. P. Sear "Nucleation: theory and applications to protein solutions and colloidal suspensions" *J. Phys.: Condens. Matter* **19** 033101 (2007).

[19] M. N. A. Karlsson, K. Deppert, L. S. Karlsson "Compaction of agglomerates of aerosol nanoparticles: A compilation of experimental data" *J Nanopart Res* **7** pp. 43–49 (2005).

[20] W. C. Hinds "Properties, behaviour and Measurement of airborne particles" **30** pp. 243-256 (2008).

[21] E. O. Knutson, K. T. Whitby "Aerosol classification by electric mobility: apparatus, theory, and applications" *Journal of Aerosol Science* **6** pp. 443-451 (1975).

[22] K. Bellmann, U. W. Pohl, et.al. "Controlling the morphology transition between step-flow growth and step-bunching growth" *Journal of Crystal Growth* **478** (2017).

[23] F. Kai "Growth Dynamics of Semiconductor Nanostructures by MOCVD" pp. 1654-2312 (2009).

[24] Xu-Q. Shen et.al. "Ammonia-free high temperature metalorganic vapor phase epitaxy (AFHT-MOVPE): a new approach to high quality AlN growth" *CrystEngComm* **20** pp. 7364-7370.

[25] M. Bar-Sadan, J. Barthel, et.al. "Direct imaging of single Au atoms within GaAs nanowires" *Nano Letters* **12** pp. 2352–2356 (2012).

[26] S. N. Mohammad "Why self-catalyzed nanowires are most suitable for large-scale hierarchical integrated designs of nanowire nanoelectronics" *Journal of Applied Physics* **110** 84310 (2011).

[27] S. Sivakumar "Aerotaxy: gas-phase epitaxy of quasi 1D nanostructures" *Nanotechnology* **32** 025605 (2021).

[28] K. Deppert, J. O. Bovin, et.al. "A new method to fabricate size-selected compound semiconductor nanocrystals: aerotaxy" **169** pp. 13-19 (1996).